Hindawi
Journal of Chemistry
Volume 2021, Article ID 3734185, 15 pages
https://doi.org/10.1155/2021/3734185

Research Article

Novel Degree-Based Topological Descriptors of Carbon Nanotubes

M. C. Shanmukha,[1] A. Usha,[2] M. K. Siddiqui,[3] K. C. Shilpa,[4] and A. Asare-Tuah[5]

[1]*Department of Mathematics, Jain Institute of Technology, Davanagere-577003, Karnataka, India*
[2]*Department of Mathematics, Alliance School of Applied Mathematics, Alliance University, Bangalore-562106, Karnataka, India*
[3]*Department of Mathematics, Comsats University Islamabad, Lahore Campus, Lahore, Pakistan*
[4]*Department of Computer Science and Engineering, Bapuji Institute of Engineering and Technology, Davanagere-577004, Karnataka, India*
[5]*Department of Mathematics, University of Ghana, Legon, Ghana*

Correspondence should be addressed to A. Asare-Tuah; aasare-tuah@ug.edu.gh

Received 27 July 2021; Accepted 27 August 2021; Published 8 September 2021

Academic Editor: Ajaya Kumar Singh

The most significant tool of mathematical chemistry is the numerical descriptor called topological index. Topological indices are extensively used in modelling of chemical compounds to analyse the studies on quantitative structure activity/property/toxicity relationships and combinatorial library virtual screening. In this work, an attempt is made in defining three novel descriptors, namely, neighborhood geometric-harmonic, harmonic-geometric, and neighborhood harmonic-geometric indices. Also, the aforementioned three indices along with the geometric-harmonic index are tested for physicochemical properties of octane isomers using linear regression models and computed for some carbon nanotubes.

1. Introduction

The applications of graph theory are diversified in every field, but chemistry is the major area of the implementation of graph theory. In chemical graph theory, topological index plays a vital role which facilitates the chemists with a treasure of data that correlate with the structure of the chemical compound. The topological index is a numerical descriptor, defines the graph topology of the molecule, and predicts an extensive range of molecular properties 5[1–6].

From the last two decades, topological indices (TIs) are identified and used in pharmacological medicine, bio-inorganic chemistry, toxicity, and theoretical chemistry and are also used for correlation analysis [7–11].

Topological descriptors are frequently used in the discovery of drugs as they have rich datasets that give high predictive values. These descriptors give the information depending on the arrangement of atoms and their bonds of a chemical compound. They are studied for chemical compounds where, generally, the hydrogen atoms are suppressed. The originality of QSAR/QSPR models depends on physicochemical properties for chemical compounds with high degree of precision. These models depend on various factors such as selecting the suitable compounds, suitable descriptors, and suitable algorithms or tools used in model development [12]. The QSAR/QSPR analysis is based on the data obtained by the numerical descriptors. These data are used to verify whether the compound under the study is suitable for drug making as the TIs provide computational data about the compound. Considering the information of the compound, QSAR/QSPR/QSTR analyses are carried out.

The TIs have increasing popularity in the field of research as they involve only computation without performing any physical experiment. Recent years have proved considerable attention in TIs as the effects of an atomic type and group efforts are considered in QSAR/QSPR modelling [13–15]. Distance-based TIs are used in QSAR analysis,

while chirality descriptors are introduced based on molecular graphs [16].

Alkanes are acyclic saturated hydrocarbons in which carbons and hydrogens are arranged in a tree-like structure. The main use of alkanes is found in crude oil such as petroleum, cooking gas, pesticides, and drug synthesis. The compounds that contain absolutely the same number of atoms but their arrangement differs are termed as isomers. A study is carried out for eighteen octane isomers (refer Figure 1).

A structure whose size is between the microscopic and molecular structure is referred to as a nanostructure. There are different types of nanostructures, namely, nanocages, nanocomposites, nanoparticles, nanofabrics, etc. In the recent years, nanostructures have attracted a lot of researchers in the areas of biology, chemistry, and medicines. Topological indices of nanostructures can be studied from [17–24]. The nanostructures made of carbons with cylindrical shape are carbon nanotubes (CNTs). They have a similar structure to that of a fullerene and graphene except their cylindrical shape. The shape of fullerene is as that of a football or basketball design where hexagons are connected.

In 1991, Iijima [25] used carbon nanotubes that have attracted many researchers in nanoscience and nanotechnology worldwide. As they have exotic properties, they are widely used in both research and applications. Nanotubes have a distinctive structure with remarkable mechanical and electrical properties. In case of carbon nanotubes, the hexagons are surrounded by squares, and each of these patterns is linearly arranged. Carbon nanotubes reveal exceptional electrical conductivity and possess wonderful tensile strength and thermal conductivity as they have nanostructures in which the carbon atoms are strongly connected.

Carbon nanotubes have applications in orthopaedic implants, especially in total hip replacement and other treatments pertaining to bone-related ailments. They are used as a grouting agent placed between the prosthesis and the bone as a part of their therapeutic use. The CNTs are used in biomedical fields because of their structural stiffness and effective optical absorption from UV to IR. Also, they can be altered chemically which are expected to be useful in many fields of technology such as electronics, composited materials, and carbon fibres. They have incredible applications in the field of materials science [26]. When the hexagonal lattice is rolled in different directions, it looks like single-wall carbon nanotubes have spiral shape and translational symmetry along the tube axis. It has rotational symmetry along its own axis. Even though nanotubes have favourable applications in a variety of fields, their large-scale production has been restricted. The main constraint that obstructs their use lies in difficulty in controlling their structure, impurities, and poor process ability. To enhance their usage, they have grabbed the attention especially in the formation of composites with polymers.

There are two types of configurations in the arrangement of nanotubes, namely, zigzag and armchair. In the zigzag configuration, the hexagons are placed one below the other linearly, whereas in the armchair configuration, they are placed next to each other. This gives two different types of configurations with different terminologies discussed now. To explain the structure of a nanotube that is infinitely long, we imagine it to be cut open by a parallel axis and placed on a plane. Then, the atoms and bonds coincide with an imaginary graphene sheet. The length of the two atoms on opposite edges of the strip corresponds to circumference of the cylindrical graphene sheet [27–29].

The main objectives of this work are as follows:

To define novel indices

To discuss the physical and chemical applicability of octane isomers using regression models

To compute defined indices for carbon nanotubes such as $C_4C_8(S)$, $C_4C_8(R)$, and H-naphthalenic nanosheets

Let $G = (V, E)$ be a graph with a vertex set $V(G)$ and an edge set $E(G)$ such that $|V(G)| = n$ and $|E(G)| = m$. For standard graph terminologies and notations, refer to [30, 31].where (u, v) is an element of $E(G)$, d_u represents the degree of the vertex u, and S_u represents the neighborhood degree of the vertex u.

Definition 1. Recently, Usha et al. [32] defined the geometric-harmonic (GH) index, inspired by Vukicevic and Furtula [33] in designing the GA index:

$$\mathrm{GH}(G) = \sum \frac{(d_u + d_v)\sqrt{d_u \cdot d_v}}{2}. \tag{1}$$

Motivated by the above work, in this paper, an attempt is made to define three novel indices based on degree and neighborhood degree, namely, harmonic-geometric (HG), neighborhood geometric-harmonic (NGH), and neighborhood harmonic-geometric (NHG) indices. They are defined as follows:

$$\begin{aligned} \mathrm{HG}(G) &= \sum \frac{2}{(d_u + d_v)\sqrt{d_u \cdot d_v}}, \\ \mathrm{NGH}(G) &= \sum \frac{(S_u + S_v)\sqrt{S_u \cdot S_v}}{2}, \\ \mathrm{NHG}(G) &= \sum \frac{2}{(S_u + S_v)\sqrt{S_u \cdot S_v}}, \end{aligned} \tag{2}$$

1.1. Chemical Applicability of GH, NGH, HG, and NHG Indices. In this section, a linear regression model of four physical properties is presented for GH, NGH, HG, and NHG indices. The physical properties such as entropy (S), acentric factor (AF), enthalpy of vaporization (HVAP), and standard enthalpy of vaporization (DHVAP) of octane isomers have shown good correlation with the indices considered in the study. The GH, HG, NGH, and NHG indices are tested for the octane isomers' database available at https://www.moleculardescriptors.eu/dataset.htm. The GH, HG, NGH, and NHG indices are computed and tabulated in columns 6, 7, 8, and 9 of Table 1.

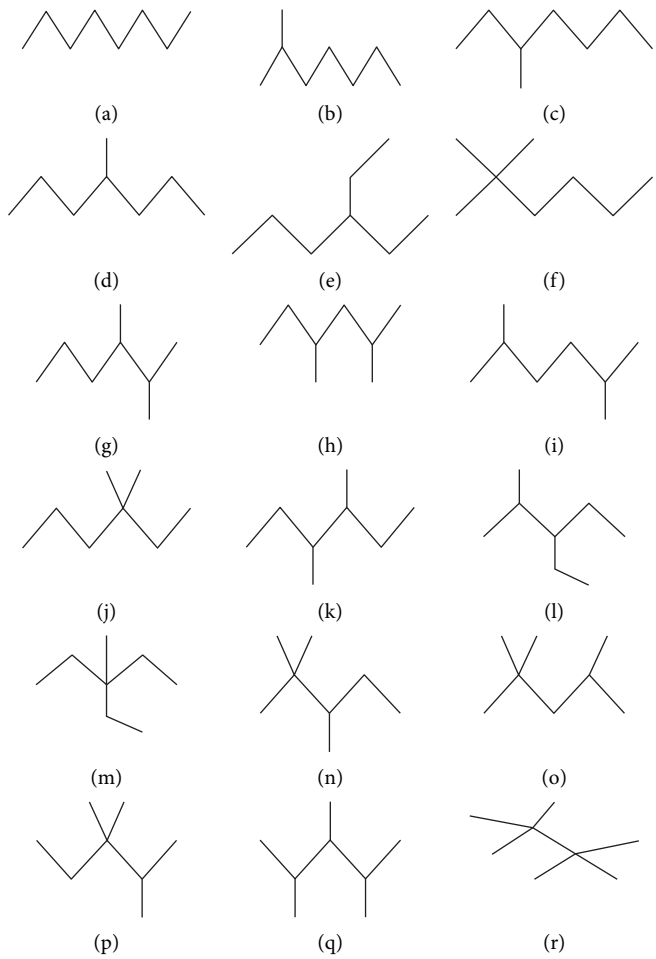

Figure 1: (a) *n*-Octane, (b) 2-methylheptane, (c) 3-methylheptane, (d) 4-methylheptane, (e) 3-ethylhexane, (f) 2,2-dimethylhexane, (g) 2,3-dimethylhexane, (h) 2,4-dimethylhexane, (i) 2,5-dimethylhexane, (j) 3,3-dimethylhexane, (k) 3,4-dimethylhexane, (l) 3-ethyl-2-methylpentane, (m) 3-ethyl-3-methylpentane, (n) 2,2,3-trimethylpentane, (o) 2,2,4-trimethylpentane, (p) 2,3,3-trimethylpentane, (q) 2,3,4-trimethylpentane, and (r) 2,2,3,3-trimethylbutane.

Table 1: Experimental values of *S*, AF, HVAP, and DHVAP and the corresponding values of the GH index, HG index, NGH index, and NHG index of octane isomers.

Alkane	*S*	AF	HVAP	DHVAP	GH	NGH	HG	NHG
n-Octane	111.700	0.398	73.190	9.915	24.423	84.496	2.193	0.679
2-Methylheptane	109.800	0.378	70.300	9.484	27.173	98.746	1.962	0.573
3-Methylheptane	111.300	0.371	71.300	9.521	27.954	107.475	2.058	0.568
4-Methylheptane	109.300	0.372	70.910	9.483	27.954	113.356	2.058	0.600
3-Ethylhexane	109.400	0.362	71.700	9.476	28.735	131.941	2.154	0.476
2,2-Dimethylhexane	103.400	0.339	67.700	8.915	33.607	122.970	1.689	0.471
2,3-Dimethylhexane	108.000	0.348	70.200	9.272	31.637	110.622	1.862	0.498
2,4-Dimethylhexane	107.000	0.344	68.500	9.029	30.885	123.236	1.827	0.474
2,5-Dimethylhexane	105.700	0.357	68.600	9.051	32.248	133.242	1.731	0.469
3,3-Dimethylhexane	104.700	0.323	68.500	8.973	35.213	151.398	1.829	0.449
3,4-Dimethylhexane	106.600	0.340	70.200	9.316	32.418	117.701	1.958	0.578
2-Methyl-3-ethylpentane	106.100	0.332	69.700	9.209	32.418	176.111	1.958	0.342
3-Methyl-3-ethylpentane	101.500	0.307	69.300	9.081	36.820	149.222	1.968	0.377
2,2,3-Trimethylpentane	101.300	0.301	67.300	8.826	38.834	164.366	1.606	0.338
2,2,4-Trimethylpentane	104.100	0.305	64.870	8.402	36.537	155.874	1.459	0.358
2,3,3-Trimethylpentane	102.100	0.293	68.100	8.897	39.659	141.657	1.649	0.462
2,3,4-Trimethylpentane	102.400	0.317	68.370	9.014	35.321	168.797	1.666	0.390
2,2,3,3-Trimethylbutane	93.060	0.255	66.200	8.410	46.000	223.620	1.263	0.227

Using the method of least squares, the linear regression models for S, AF, HVAP, and DHVAP are fitted using the data of Table 1.

The fitted models for the GH index are

$$S = 133.078\,(\pm\ 1.82) - 0.833\,(\pm\ 0.054)\mathrm{GH}, \quad (3)$$

$$\text{acentric factor} = 0.557\,(\pm\ 0.009) - 0.007\,(\pm\ 0.000)\mathrm{GH}, \quad (4)$$

$$\mathrm{HVAP} = 79.613\,(\pm\ 1.878) - 0.315\,(\pm\ 0.056)\mathrm{GH}, \quad (5)$$

$$\mathrm{DHVAP} = 11.273\,(\pm\ 0.285) - 0.065\,(\pm\ 0.008)\mathrm{GH}. \quad (6)$$

The fitted models for the HG index are

$$S = 76.608\,(\pm\ 4.486) + 15.766\,(\pm\ 2.435)\mathrm{HG}, \quad (7)$$

$$\text{acentric factor} = 0.114\,(\pm\ 0.037) + 0.121\,(\pm\ 0.020)\mathrm{HG}, \quad (8)$$

$$\mathrm{HVAP} = 54.960\,(\pm\ 1.356) + 7.773\,(\pm\ 0.736)\mathrm{HG}, \quad (9)$$

$$\mathrm{DHVAP} = 6.428\,(\pm\ 0.249) + 1.477\,(\pm\ 0.135)\mathrm{HG}. \quad (10)$$

The fitted models for the NGH index are

$$S = 121.77\,(\pm\ 2.35) - 0.119\,(\pm\ 0.017)\mathrm{NGH}, \quad (11)$$

$$\text{acentric factor} = 0.465\,(\pm\ 0.018) - 0.001\,(\pm\ 0.000)\mathrm{NGH}, \quad (12)$$

$$\mathrm{HVAP} = 75.007\,(\pm\ 1.552) - 0.043\,(\pm\ 0.011)\mathrm{NGH}, \quad (13)$$

$$\mathrm{DHVAP} = 10.363\,(\pm\ 0.257) - 0.009\,(\pm\ 0.002)\mathrm{NGH}. \quad (14)$$

The fitted models for the NHG index are

$$S = 89.524\,(\pm\ 2.505) + 34.35\,(\pm\ 5.271)\mathrm{NHG}, \quad (15)$$

$$\text{acentric factor} = 0.207\,(\pm\ 0.018) + 0.277\,(\pm\ 0.038)\mathrm{NHG}, \quad (16)$$

$$\mathrm{HVAP} = 62.667\,(\pm\ 1.352) + 14.044\,(\pm\ 2.846)\mathrm{NHG}, \quad (17)$$

$$\mathrm{DHVAP} = 7.793\,(\pm\ 0.219) + 2.882\,(\pm\ 0.460)\mathrm{NHG}. \quad (18)$$

Note: in equations (3)–(18), the errors of the regression coefficients are represented within brackets.

Tables 2–5 and Figures 2–5 show the correlation coefficient and residual standard error for the regression models of four physical properties with GH, HG, NGH, and NHG indices.

From Table 2 and Figure 2, it is obvious that the GH index highly correlates with the acentric factor and the correlation coefficient $|r| = 0.987$. Also, the GH index has good correlation coefficient $|r| = 0.968$ with entropy, $|r| = 0.815$ with HVAP, and $|r| = 0.885$ with DHVAP.

From Table 3 and Figure 3, it is noticed that the HG index highly correlates with DHVAP and the correlation coefficient $r = 0.939$. Also, the HG index has good correlation coefficient $r = 0.85$ with entropy, $r = 0.833$ with the acentric factor, and $r = 0.935$ with HVAP.

From Table 4 and Figure 4, it is clear that the NGH index highly correlates with the acentric factor and the correlation coefficient $|r| = 0.877$. Also, the NGH index has good correlation coefficient $|r| = 0.873$ with entropy, $|r| = 0.695$ with HVAP, and $|r| = 0.778$ with DHVAP.

From Table 5 and Figure 5, it is clear that the NHG index highly correlates with the acentric factor and the correlation coefficient $r = 0.877$. Also, the NHG index has good correlation coefficient $r = 0.852$ with entropy, $r = 0.777$ with HVAP, and $r = 0.843$ with DHVAP.

2. GH, NGH, HG, and NHG Indices of $C_4C_8(S)$, $C_4C_8(R)$, and H-Naphthalenic Nanosheets

2.1. Results for the $C_4C_8(S)$ Nanosheet. The alternating pattern of 4 carbon atoms forming squares and 8 carbon atoms forming octagons constitutes the $\mathrm{TUC}_4\mathrm{C}_8(S)[a,b]$ nanosheet.

In this section, GH, HG, NGH, and NHG indices of the $C_4C_8(S)$ nanosheet are computed. The pattern of carbon atoms gives rise to two types of nanosheets, namely, $T^1[a,b]$ and $T^2[a,b]$. The 2-dimensional nanosheet is represented by $T^1[a,b]$, where a and b are parameters (Figure 6). In $T^1[a,b]$, C_4 acts as a square, while C_8 is an octagon in which a and b represent the column and row, respectively. Figure 7 depicts the type $1-C_4C_8(S)$ nanosheet. The number of vertices of the $C_4C_8(S)$ nanosheet is $8ab$, and the number of edges is $12ab - 2a - 2b$.

The edge partition of the $T^1[a,b]$ nanosheet based on the degree of vertices is detailed in Table 6.

Theorem 1. *Let $T^1[a,b]$ be an (a,b)-dimensional nanosheet; then, GH and HG indices are equal to*

$$\mathrm{GH}\left(T^1[a,b]\right) = 108ab - \frac{4938}{125}a - \frac{4938}{125}b + \frac{376}{125},$$
$$\mathrm{HG}\left(T^1[a,b]\right) = \frac{4}{3}ab + \frac{33}{125}a + \frac{33}{125}b + \frac{69}{500}. \quad (19)$$

Proof. Using Table 6, the definitions of GH and HG indices are as follows:

Table 2: Parameters of regression models for the GH index.

Physical properties	Value of the correlation coefficient	Residual standard error
Entropy	−0.968	1.17
Acentric factor	−0.987	0.0059
HVAP	−0.815	1.21
DHVAP	−0.885	0.184

Table 3: Parameters of regression models for the HG index.

Physical properties	Value of the correlation coefficient	Residual standard error
Entropy	0.85	2.448
Acentric factor	0.833	0.020
HVAP	0.935	0.74
DHVAP	0.939	0.136

Table 4: Parameters of regression models for the NGH index.

Physical properties	Value of the correlation coefficient	Residual standard error
Entropy	−0.873	2.274
Acentric factor	−0.877	0.0176
HVAP	−0.695	1.502
DHVAP	−0.778	0.248

Table 5: Parameters of regression models for the NHG index.

Physical properties	Value of the correlation coefficient	Residual standard error
Entropy	0.852	2.436
Acentric factor	0.877	0.018
HVAP	0.777	1.315
DHVAP	0.843	0.213

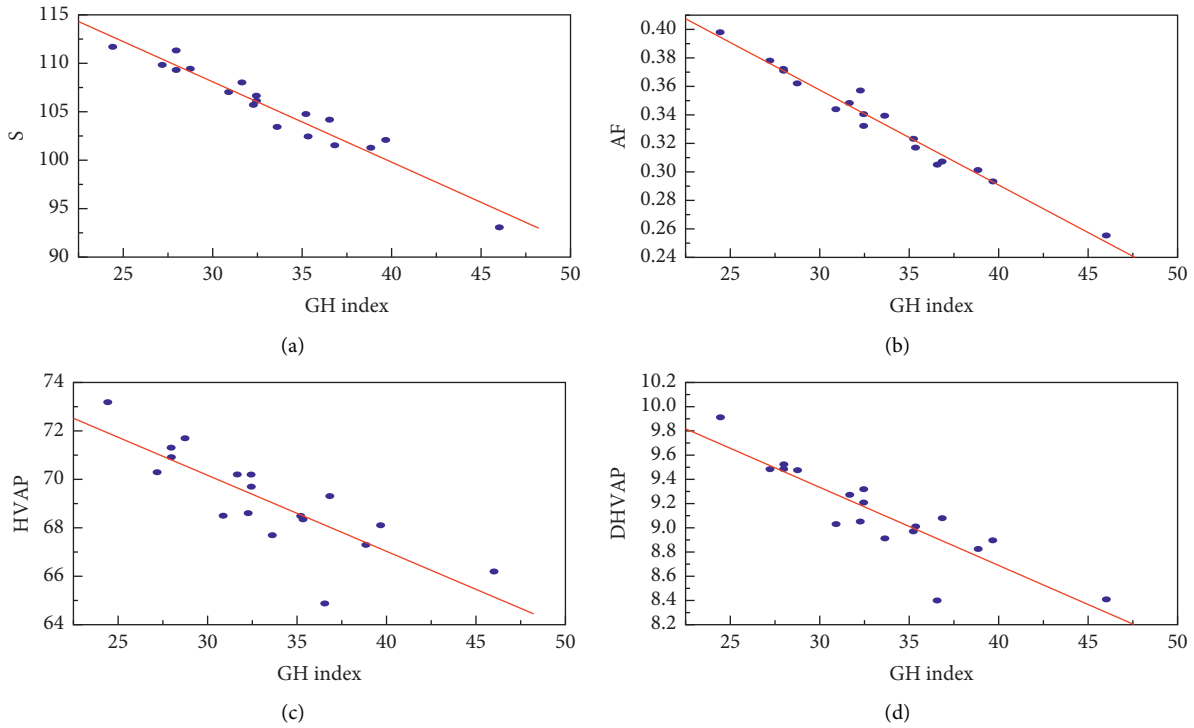

Figure 2: Scatter diagram of physical properties *S*, AF, HVAP, and DHVAP with the GH index.

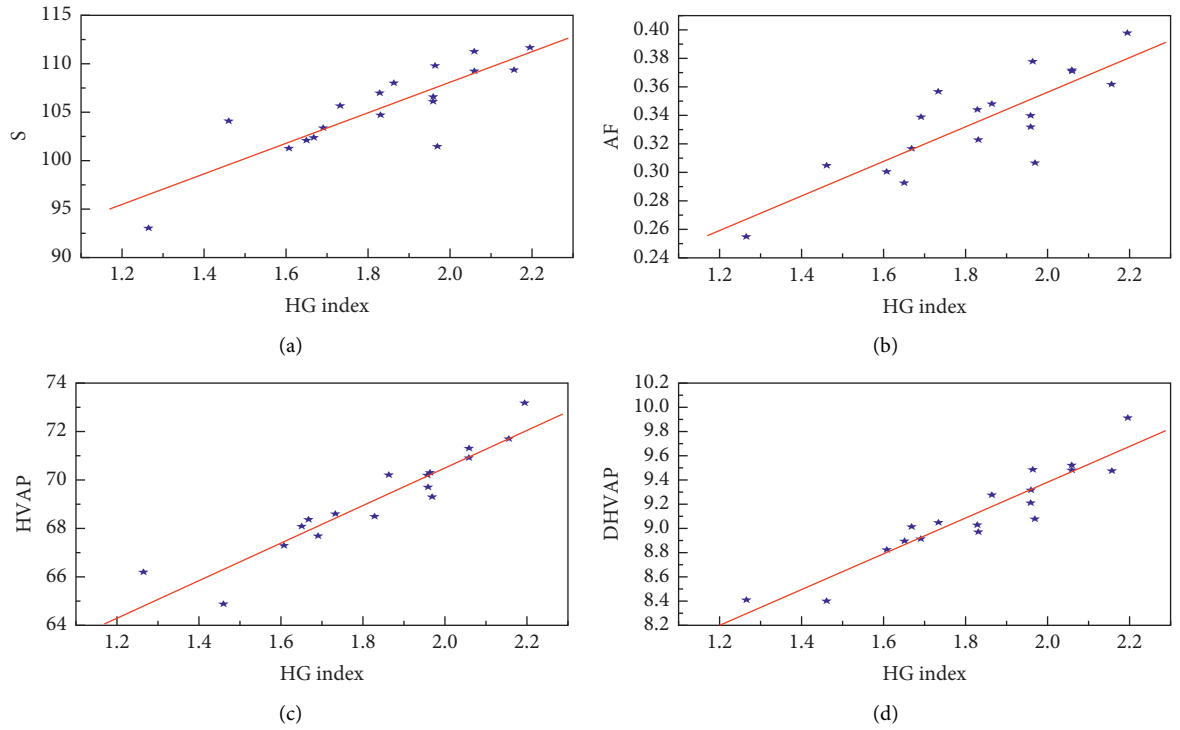

Figure 3: Scatter diagram of physical properties *S*, AF, HVAP, and DHVAP with the HG index.

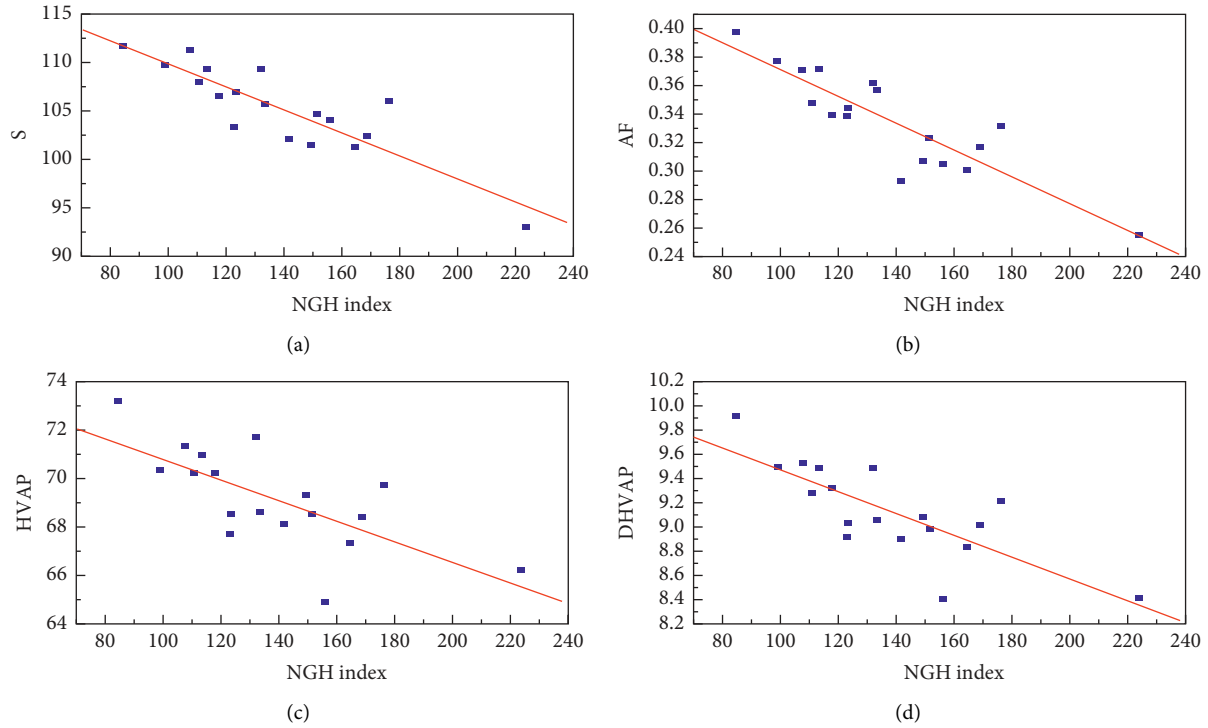

Figure 4: Scatter diagram of physical properties *S*, AF, HVAP, and DHVAP with the NGH index.

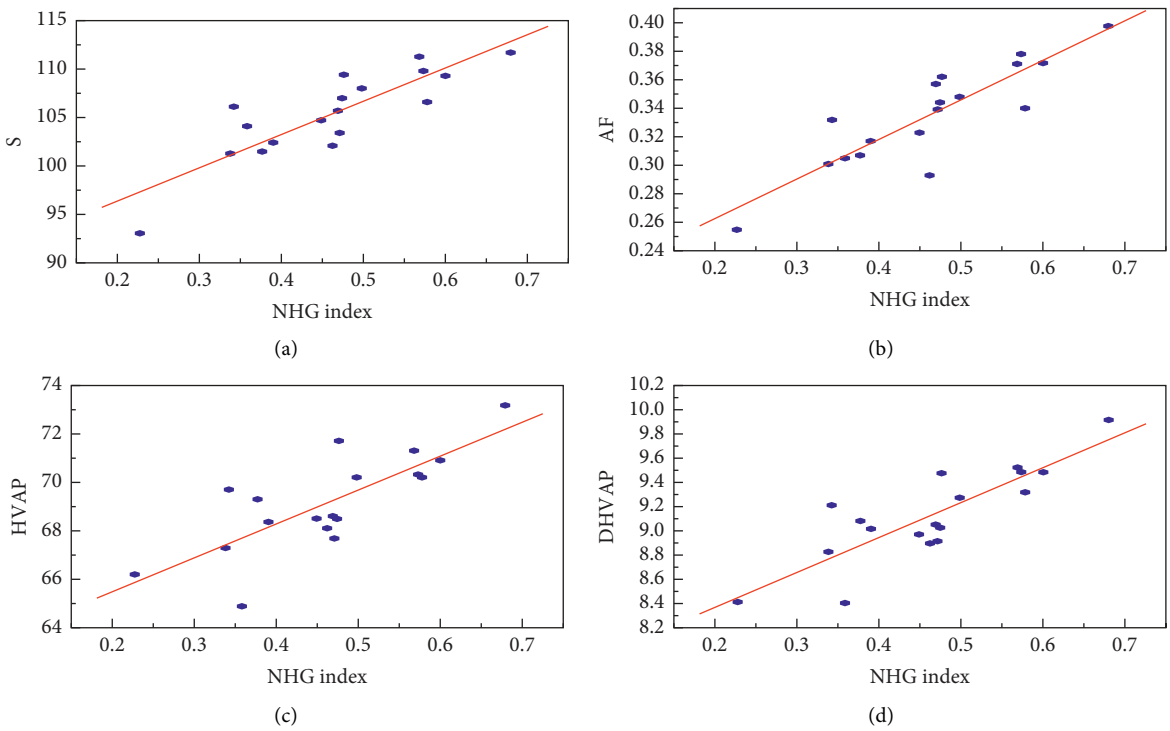

Figure 5: Scatter diagram of physical properties S, AF, HVAP, and DHVAP with the NHG index.

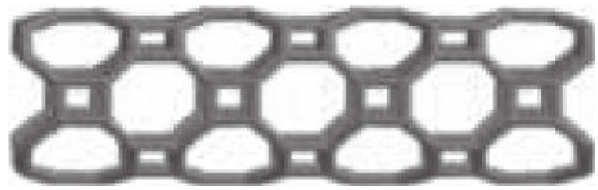

Figure 6: A $TUC_4C_8(S)[a, b]$ nanotube.

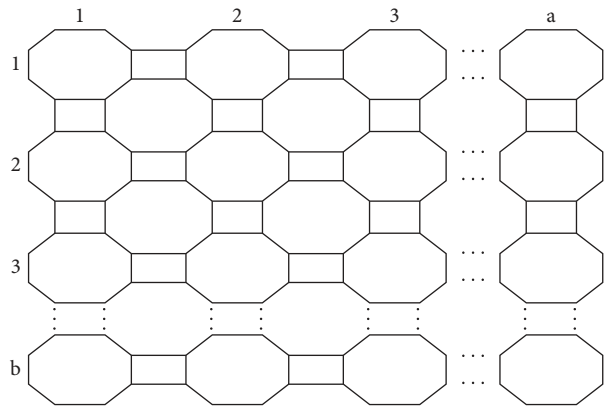

Figure 7: Type I-$C_4C_8(S)$ nanosheet $T^1[a, b]$.

Table 6: The edge partition of $T^1[a,b]$.

(d_u, d_v) with $uv \in E(G)$	Number of edges
$(2,2)$	$2(a+b+2)$
$(2,3)$	$4a+4b-8$
$(3,3)$	$12ab-8a-8b+4$

$$\begin{aligned}
\mathrm{GH}\left(T^1[a,b]\right) &= \sum_{uv\in E(G)} \frac{(d_u+d_v)\sqrt{d_u\times d_v}}{2} \\
&= (2a+2b+4)\left\{\frac{(2+2)(\sqrt{2\times 2})}{2}\right\} + (4a+4b-8)\left\{\frac{(2+3)(\sqrt{2\times 3})}{2}\right\} \\
&\quad + (12ab-8a-8b+4)\left\{\frac{(2+3)(\sqrt{2\times 3})}{2}\right\} \\
\mathrm{GH}\left(T^1[a,b]\right) &= 108ab - \frac{4938}{125}a - \frac{4938}{125}b + \frac{376}{125}, \\
\mathrm{HG}\left(T^1[a,b]\right) &= \sum_{uv\in E(G)} \frac{2}{(d_u+d_v)\sqrt{d_u\times d_v}} \\
&= (2a+2b+4)\left\{\frac{2}{(2+2)(\sqrt{2\times 2})}\right\} + (4a+4b-8)\left\{\frac{2}{(2+3)(\sqrt{2\times 3})}\right\} \\
&\quad + (12ab-8a-8b+4)\left\{\frac{2}{(2+3)(\sqrt{2\times 3})}\right\} \\
\mathrm{HG}\left(T^1[a,b]\right) &= \frac{4}{3}ab + \frac{33}{125}a + \frac{33}{125}b + \frac{69}{500}.
\end{aligned} \tag{20}$$

□

The edge partition of the $T^1[a,b]$ nanosheet based on the neighborhood degree of vertices is detailed in Table 7.

Theorem 2. *Let $T^1[a,b]$ be an (a,b)-dimensional nanosheet; then, NGH and NHG indices are equal to*

$$\begin{aligned}
\mathrm{NGH}\left(T^1[a,b]\right) &= 972ab - \frac{251531}{500}a - \frac{251531}{500}b + \frac{159121}{1000}, \\
\mathrm{NHG}\left(T^1[a,b]\right) &= \frac{37}{250}ab + \frac{91}{1000}a + \frac{91}{1000}b + \frac{157}{1000}.
\end{aligned} \tag{21}$$

Proof. Using Table 7, the definitions of NGH and NHG indices are as follows:

Table 7: Edge partition of $T^1[a,b]$ for neighborhood degree-based vertices.

(S_u, S_v) with $uv \in E(G)$	Number of edges
(4, 4)	4
(4, 5)	8
(5, 5)	$2a + 2b - 8$
(5, 8)	$4a + 4b - 8$
(8, 8)	$2a + 2b - 4$
(8, 9)	$4a + 4b - 8$
(9, 9)	$12ab - 14a - 14b + 16$

$$\begin{aligned}
\mathrm{NGH}\left(T^1[a,b]\right) &= \sum_{uv\in E(G)} \frac{(S_u + S_v)\sqrt{S_u \times S_v}}{2} \\
&= 4\left\{\frac{(4+4)(\sqrt{4\times 4})}{2}\right\} + 8\left\{\frac{(4+5)(\sqrt{4\times 5})}{2}\right\} + (2a+2b-8)\left\{\frac{(5+5)(\sqrt{5\times 5})}{2}\right\} + (4a+4b-8) \\
&\cdot \left\{\frac{(5+8)(\sqrt{5\times 8})}{2}\right\} + (2a+2b-4)\left\{\frac{(8+8)(\sqrt{8\times 8})}{2}\right\} + (4a+4b-8)\left\{\frac{(8+9)(\sqrt{8\times 9})}{2}\right\} \\
&+ (12ab-14a-14b+16)\left\{\frac{(9+9)(\sqrt{9\times 9})}{2}\right\} \\
\mathrm{NGH}\left(T^1[a,b]\right) &= 972ab - \frac{251531}{500}a - \frac{251531}{500}b + \frac{159121}{1000}, \\
\mathrm{NHG}\left(T^1[a,b]\right) &= \sum_{uv\in E(G)} \frac{(S_u + S_v)\sqrt{S_u \times S_v}}{2} \\
&= 4\left\{\frac{2}{(4+4)(\sqrt{4\times 4})}\right\} + 8\left\{\frac{2}{(4+5)(\sqrt{4\times 5})}\right\} + (2a+2b-8)\left\{\frac{2}{(5+5)(\sqrt{5\times 5})}\right\} + (4a+4b-8) \\
&\cdot \left\{\frac{2}{(5+8)(\sqrt{5\times 8})}\right\} + (2a+2b-4)\left\{\frac{2}{(8+8)(\sqrt{8\times 8})}\right\} + (4a+4b-8)\left\{\frac{2}{(8+9)(\sqrt{8\times 9})}\right\} \\
&+ (12ab-14a-14b+16)\left\{\frac{2}{(9+9)(\sqrt{9\times 9})}\right\} \\
\mathrm{NHG}\left(T^1[a,b]\right) &= \frac{37}{250}ab + \frac{91}{1000}a + \frac{91}{1000}b + \frac{157}{1000}.
\end{aligned} \tag{22}$$

□

2.2. Results for the $C_4C_8(R)$ Nanosheet. This structure is formed by 4 carbon atoms forming a rhombus that are linearly bridged by edges whose sequence looks like 4 rhombuses connected by 4 edges row and column wise resulting in an alternating pattern of rhombuses and octagons and is represented as $T^2[a,b]$. The 2-dimensional lattice of the $\mathrm{TUC}_4\mathrm{C}_8(R)[a,b]$ nanosheet, where a and b are parameters, is shown in Figure 8. Figure 9 shows the type $2 - \mathrm{C}_4\mathrm{C}_8(R)$ nanosheet. In the following theorem, GH, HG, NGH, and NHG indices of this nanosheet are computed. The number of vertices of the type-2 structure is $4ab + 4(a + b) + 4$, and the number of edges is $6ab + 5a + 5b + 4$.

The edge partition of the $T^2[a,b]$ nanosheet for degree-based vertices is detailed in Table 8.

Theorem 3. *Let $T^2[a,b]$ be an (a,b)-dimensional nanosheet; then, GH and HG indices are equal to*

$$\begin{aligned}
\mathrm{GH}\left(T^2[a,b]\right) &= 54ab + \frac{669}{20}a + \frac{669}{20}b + 16, \\
\mathrm{HG}\left(T^2[a,b]\right) &= \frac{2}{3}ab + \frac{191}{250}a + \frac{191}{250}b + 1.
\end{aligned} \tag{23}$$

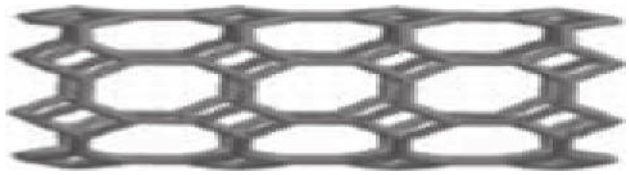

Figure 8: A $TUC_4C_8(R)[a,b]$ nanotube.

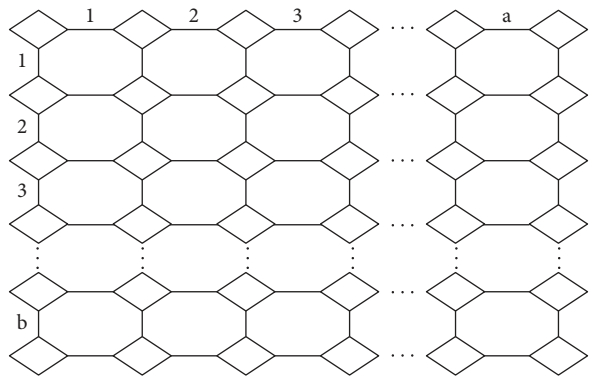

Figure 9: Type II-$C_4C_8(R)$ nanosheet $T^2[a,b]$.

Table 8: Edge partition of $T^2[a,b]$.

(d_u, d_v) with $uv \in E(G)$	Number of edges
$(2,2)$	4
$(2,3)$	$4(a+b)$
$(3,3)$	$6ab+a+b$

Proof. Using Table 8, the definitions of GH and HG indices are as follows:

$$\begin{aligned}
\mathrm{GH}\left(T^2[a,b]\right) &= \sum_{uv\in E(G)} \frac{(d_u+d_v)\sqrt{d_u\times d_v}}{2} \\
&= 4\left\{\frac{(2+2)(\sqrt{2\times 2})}{2}\right\} + (4a+4b)\left\{\frac{(2+3)(\sqrt{2\times 3})}{2}\right\} + (6ab+a+b)\left\{\frac{(3+3)(\sqrt{3\times 3})}{2}\right\} \\
\mathrm{GH}\left(T^2[a,b]\right) &= 54ab + \frac{669}{20}a + \frac{669}{20}b + 16, \\
\mathrm{HG}\left(T^2[a,b]\right) &= \sum_{uv\in E(G)} \frac{2}{(d_u+d_v)\sqrt{d_u\times d_v}} \\
&= 2\left\{\frac{2}{(2+2)(\sqrt{2\times 2})}\right\} + (4a+4b)\left\{\frac{2}{(2+3)(\sqrt{2\times 3})}\right\} + (6ab+a+b)\left\{\frac{2}{(3+3)(\sqrt{3\times 3})}\right\} \\
\mathrm{HG}\left(T^2[a,b]\right) &= \frac{2}{3}ab + \frac{191}{250}a + \frac{191}{250}b + 1.
\end{aligned} \tag{24}$$

□

The edge partition of the $T^2[a,b]$ nanosheet based on the neighborhood degree of vertices is detailed in Table 9.

Theorem 4. *Let $T^2[a,b]$ be an (a,b)-dimensional nanosheet; then, NGH and NHG indices are equal to*

$$\begin{aligned}\mathrm{NGH}\left(T^2[a,b]\right) &= 486ab + \frac{20549}{100}a + \frac{20549}{100}b + \frac{21549}{500},\\ \mathrm{NHG}\left(T^2[a,b]\right) &= \frac{37}{500}ab + \frac{107}{1000}a + \frac{107}{1000}b + \frac{19}{100}.\end{aligned} \tag{25}$$

Table 9: Edge partition of $T^2[a,b]$.

(S_u, S_v) with $uv \in E(G)$	Number of edges
$(5,5)$	4
$(5,8)$	8
$(6,8)$	$4a + 4b - 8$
$(8,8)$	$2a + 2b + 4$
$(8,9)$	$4a + 4b - 8$
$(9,9)$	$6ab - 5a - 5b + 4$

Proof. Using Table 9, the definitions of NGH and NHG indices are as follows:

$$\begin{aligned}\mathrm{NGH}\left(T^2[a,b]\right) &= \sum_{uv\in E(G)} \frac{(S_u + S_v)\sqrt{S_u \times S_v}}{2}\\ &= 4\left\{\frac{(5+5)(\sqrt{5\times 5})}{2}\right\} + 8\left\{\frac{(5+8)(\sqrt{5\times 8})}{2}\right\} + (4a+4b-8)\left\{\frac{(6+8)(\sqrt{6\times 8})}{2}\right\} + (2a+2b+4)\\ &\quad\cdot\left\{\frac{(8+8)(\sqrt{8\times 8})}{2}\right\} + (4a+4b-8)\left\{\frac{(8+9)(\sqrt{8\times 9})}{2}\right\} + (6ab-5a-5b+4)\left\{\frac{(9+9)(\sqrt{9\times 9})}{2}\right\}\\ \mathrm{NGH}\left(T^2[a,b]\right) &= 486ab + \frac{20549}{100}a + \frac{20549}{100}b + \frac{21549}{500},\\ \mathrm{NHG}\left(T^2[a,b]\right) &= \sum_{uv\in E(G)} \frac{2}{(S_u + S_v)\sqrt{S_u \times S_v}}\\ &= 4\left\{\frac{2}{(5+5)(\sqrt{5\times 5})}\right\} + 8\left\{\frac{2}{(5+8)(\sqrt{5\times 8})}\right\} + (4a+4b-8)\left\{\frac{2}{(6+8)(\sqrt{6\times 8})}\right\} + (2a+2b+4)\\ &\quad\cdot\left\{\frac{2}{(8+8)(\sqrt{8\times 8})}\right\} + (4a+4b-8)\left\{\frac{2}{(8+9)(\sqrt{8\times 9})}\right\} + (6ab-5a-5b+4)\left\{\frac{2}{(9+9)(\sqrt{9\times 9})}\right\}\\ \mathrm{NHG}\left(T^2[a,b]\right) &= \frac{37}{500}ab + \frac{107}{1000}a + \frac{107}{1000}b + \frac{19}{100}.\end{aligned} \tag{26}$$

□

2.3. Results for the H-Naphthalenic Nanosheet. Carbon atoms bonded in the form of a hexagonal structure constitute carbon nanotubes. They are peri-condensed benzenoids which mean three or more rings share the same atoms. H-Naphthalenic nanosheet is constituted by the alternating sequence of squares C_4, hexagons C_6, and octagons C_8 and is represented as $T^3[a,b]$, where a and b are the parameters. The number of vertices of the H-naphthalenic nanosheet is $10ab$, and the edges are $15ab - 2a - 2b$. The GH, HG, NGH, and NHG indices of this nanosheet are computed; see Figure 10.

The edge partition of the $T^3[a,b]$ nanosheet based on the degree of vertices is detailed in Table 10.

Theorem 5. *Let $T^3[a,b]$ be an (a,b)-dimensional nanosheet; then, GH and HG indices are equal to*

$$\begin{aligned}\mathrm{GH}\left(T^3[a,b]\right) &= 135ab - \frac{4101}{100}a - \frac{7901}{200}b + \frac{301}{100},\\ \mathrm{HG}\left(T^3[a,b]\right) &= \frac{1667}{1000}ab + \frac{39}{200}a + \frac{33}{125}b + \frac{69}{1500}.\end{aligned} \tag{27}$$

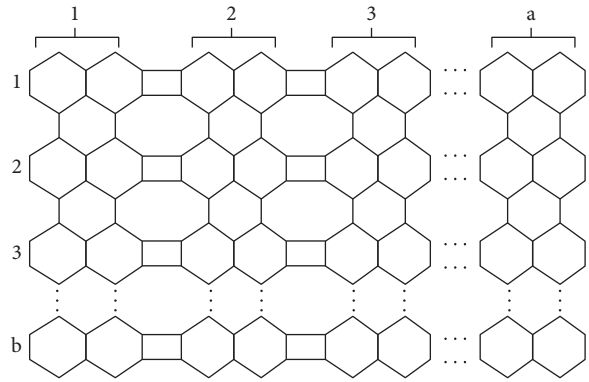

Figure 10: An H-naphthalenic nanosheet $T^3[a,b]$.

Table 10: The details of edges and types of the $T^3[a,b]$ nanosheet based on the degree of vertices.

(d_u, d_v) with $uv \in E(G)$	Number of edges
$(2,2)$	$2a+4$
$(2,3)$	$8a+4b-8$
$(3,3)$	$15ab-10a-8b+4$

Proof. Using Table 10, the definitions of GH and HG indices are as follows:

$$\begin{aligned}
\mathrm{GH}\left(T^3[a,b]\right) &= \sum_{uv\in E(G)} \frac{(d_u+d_v)\sqrt{d_u\times d_v}}{2} \\
&= (2b+4)\left\{\frac{(2+2)(\sqrt{2\times 2})}{2}\right\} + (8a+8b-8)\left\{\frac{(2+3)(\sqrt{2\times 3})}{2}\right\} \\
&\quad + (15ab-10a-8b+4)\left\{\frac{(3+3)(\sqrt{3\times 3})}{2}\right\} \\
\mathrm{GH}\left(T^3[a,b]\right) &= 135ab - \frac{4101}{100}a - \frac{7901}{200}b + \frac{301}{100}. \\
\mathrm{HG}\left(T^3[a,b]\right) &= \sum_{uv\in E(G)} \frac{2}{(d_u+d_v)\sqrt{d_u\times d_v}} \\
&= (2b+4)\left\{\frac{2}{(2+2)(\sqrt{2\times 2})}\right\} + (8a+8b-8)\left\{\frac{2}{(2+3)(\sqrt{2\times 3})}\right\} \\
&\quad + (15ab-10a-8b+4)\left\{\frac{2}{(3+3)(\sqrt{3\times 3})}\right\} \\
\mathrm{HG}\left(T^3[a,b]\right) &= \frac{1667}{1000}ab + \frac{39}{200}a + \frac{33}{125}b + \frac{69}{1500}.
\end{aligned} \tag{28}$$

□

Table 11: Edge partition of $T^3[a,b]$.

(S_u, S_v) with $uv \in E(G)$	Number of edges
(4, 5)	8
(5, 5)	$2b-4$
(5, 7)	4
(5, 8)	$4b-4$
(6, 7)	$4a-4$
(6, 8)	$4a-4$
(7, 9)	$2a$
(8, 8)	$2a+2b-4$
(8, 9)	$4a+4b-8$
(9, 9)	$15ab-18a-14b+16$

The edge partition of the $T^3[a,b]$ nanosheet based on the neighborhood degree of vertices is detailed in Table 11.

Theorem 6. *Let $T^3[a,b]$ be an (a,b)-dimensional nanosheet; then, NGH and NHG indices are equal to*

$$\begin{aligned}\mathrm{NGH}\left(T^3[a,b]\right) &= 1215ab - \frac{11199}{20}a - \frac{251531}{500}b + \frac{17382}{125},\\ \mathrm{NHG}\left(T^3[a,b]\right) &= \frac{37}{200}ab + \frac{15}{200}a + \frac{91}{1000}b + \frac{249}{2500}.\end{aligned} \tag{29}$$

Proof. Using Table 11, the definitions of NGH and NHG indices are as follows:

$$\begin{aligned}\mathrm{NGH}\left(T^3[a,b]\right) &= \sum_{uv\in E(G)} \frac{(S_u+S_v)\sqrt{S_u\times S_v}}{2}\\ &= 8\left\{\frac{(4+5)(\sqrt{4\times 5})}{2}\right\} + (2b-4)\left\{\frac{(5+5)(\sqrt{5\times 5})}{2}\right\} + 4\left\{\frac{(5+7)(\sqrt{7\times 7})}{2}\right\} + (4b-4)\\ &\quad\cdot\left\{\frac{(5+8)(\sqrt{5\times 8})}{2}\right\} + (4a-4)\left\{\frac{(6+7)(\sqrt{6\times 7})}{2}\right\} + (4a-4)\left\{\frac{(6+8)(\sqrt{6\times 8})}{2}\right\}\\ &\quad + 2a\left\{\frac{(7+9)(\sqrt{7\times 9})}{2}\right\} + (2a+2b-4)\left\{\frac{(8+8)(\sqrt{8\times 8})}{2}\right\} + (4a+4b-8)\\ &\quad\cdot\left\{\frac{(8+9)(\sqrt{8\times 9})}{2}\right\} + (15ab-18a-14b+16)\left\{\frac{(9+9)(\sqrt{9\times 9})}{2}\right\}\\ \mathrm{NGH}\left(T^3[a,b]\right) &= 1215ab - \frac{11199}{20}a - \frac{251531}{500}b + \frac{17382}{125},\\ \mathrm{NHG}\left(T^3[a,b]\right) &= \sum_{uv\in E(G)} \frac{(S_u+S_v)\sqrt{S_u\times S_v}}{2}\\ &= 8\left\{\frac{2}{(4+5)(\sqrt{4\times 5})}\right\} + (2b-4)\left\{\frac{2}{(5+5)(\sqrt{5\times 5})}\right\} + 4\left\{\frac{2}{(5+7)(\sqrt{7\times 7})}\right\} + (4b-4)\\ &\quad\cdot\left\{\frac{2}{(5+8)(\sqrt{5\times 8})}\right\} + (4a-4)\left\{\frac{2}{(6+7)(\sqrt{6\times 7})}\right\} + (4a-4)\left\{\frac{2}{(6+8)(\sqrt{6\times 8})}\right\}\\ &\quad + 2a\left\{\frac{2}{(7+9)(\sqrt{7\times 9})}\right\} + (2a+2b-4)\left\{\frac{2}{(8+8)(\sqrt{8\times 8})}\right\} + (4a+4b-8)\\ &\quad\cdot\left\{\frac{2}{(8+9)(\sqrt{8\times 9})}\right\} + (15ab-18a-14b+16)\left\{\frac{2}{(9+9)(\sqrt{9\times 9})}\right\}\\ \mathrm{NHG}\left(T^3[a,b]\right) &= \frac{37}{200}ab + \frac{15}{200}a + \frac{91}{1000}b + \frac{249}{2500}.\end{aligned} \tag{30}$$

□

3. Conclusion

This paper is devoted to defining NGH, HG, and NHG indices, and the chemical applicability is studied for some physical and chemical properties of octane isomers using regression models including the recently introduced GH index. The GH index has a high negative correlation with acentric factor having $r = 0.987$ with a residual standard error of 0.0059. The HG index has a high positive correlation with DHVAP having $r = 0.939$ with a residual standard error of 0.136. The NGH index has a high negative correlation with acentric factor having $r = 0.877$ with a residual standard error of 0.0176. The NHG index has a high positive correlation with acentric factor having $r = 0.877$ with a residual standard error of 0.018. The applications of carbon nanotubes have considerably increased because of their excellent mechanical, thermal, and electrical properties. The novel indices introduced in this paper would be of great help to understand the physicochemical and biological properties of various compounds in addition to the existing degree-based indices.

Data Availability

The data used to support the findings of this study are cited at relevant places within the text as references.

Conflicts of Interest

The authors declare that they have no conflicts of interest.

Authors' Contributions

All authors contributed equally to this work.

References

[1] D. Bonchev, *Information Theoretic Indices for Characterization of Chemical Structures*, Research Studies Press, 1983.

[2] B. Furtula and I. Gutman, "A forgotten topological index," *Journal of Mathematical Chemistry*, vol. 53, no. 4, pp. 1184–1190, 2015.

[3] I. Gutman and O. E. Polansky, *Mathematical Concepts in Organic Chemistry*, Springer, Berlin, Germany, 2012.

[4] I. Gutman and N. Trinajstić, "Graph theory and molecular orbitals. Total φ-electron energy of alternant hydrocarbons," *Chemical Physics Letters*, vol. 17, no. 4, pp. 535–538, 1972.

[5] R. Todeschini and V. Consonni, *Handbook of Molecular Descriptors*, Wiley VCH, Weinheim, Germany, 2000.

[6] N. Trinajstic, *Chemical Graph Theory*, CRC Press, Boca Raton, FL, USA, 1992.

[7] S. Hayat, M. Imran, and J. B. Liu, "Correlation between the Esrada index and π-electron energies for benzenoid hydrocarbons with applications to boron nanotubes," *International Journal of Quantum Chemistry*, vol. 119, pp. 1–13, 2019.

[8] M. Randic, "Quantitative structure-property relationship. Boiling points of planar benzenoids," *New Journal of Chemistry*, vol. 20, pp. 1001–1009, 1996.

[9] M. C. Shanmukha, A. Usha, N. S. Basavarajappa, and K. C. Shilpa, "Novel Neighbourhood redefined First and Second Zagreb indices on Carborundum Structures," *Journal of Applied Mathematics and Computing*, vol. 66, pp. 1–14, 2020.

[10] M. C. Shanmukha, N. S. Basavarajappa, K. C. Shilpa, and A. Usha, "Degree-based topological indices on anticancer drugs with QSPR analysis," *Heliyon*, vol. 6, Article ID e04235, 2020.

[11] S. A. K. Kirmani, P. Ali, F. Azam, and P. A. Alvi, "Topological indices and QSPR/QSAR analysis of some antiviral drugs being investigated for the treatment of COVID-19 patients," *International Journal of Quantum Chemistry*, vol. 121, pp. 1–22, 2021.

[12] K. Roy, "Topological descriptors in drug design and modeling studies," *Molecular Diversity*, vol. 8, no. 4, pp. 321–323, 2004.

[13] A. T. Balaban and J. Devillers, *Topological Indices and Related Descriptors in QSAR and QSPR*, CRC Press, London, UK, 2014.

[14] J. C. Dearden, *Advances in QSAR Modeling*, Springer, Cham, Switzerland, pp. 57–88, 2017.

[15] E. Estrada, L. Torres, L. Roriguez, and I. Gutman, "An atom-bond connectivity index: modelling the enthalpy of formation of alkanes," *Indian Journal of Chemistry*, vol. 37, pp. 849–855, 1998.

[16] H. Wiener, "Structural determination of parafin boiling points," *Journal of the American Chemical Society*, vol. 69, no. 1, pp. 17–20, 1947.

[17] B. Basavangouda and S. Policepatil, "Chemical applicability of Gourava and hyper-Gourava indices," *Nanosystems: Physics, Chemistry, Mathematics*, vol. 12, pp. 142–150, 2021.

[18] P. S. R. Harisha and V. Lokesha, "M-Polynomial of valency-based topological indices of operators on titania nanotubes $TiO_2[m,n]$ networks," *Advances and Applications in Mathematical Sciences*, vol. 20, pp. 1493–1508, 2021.

[19] P. S. Hemavathi, V. Lokesha, M. Manjunath, P. S. KReddy, and R. Shruti, "Topological aspects boron triangular nanotube and boron-α nanotube," *Vladikavkaz Mathematical Journal*, vol. 22, pp. 66–77, 2020.

[20] V. Lokesha, T. Deepika, P. S. Ranjini, and I. N. Cangul, "Operations of nanostructures via SDD, ABC 4 and GA 5 indices," *Applied Mathematics and Nonlinear Sciences*, vol. 2, no. 1, pp. 173–180, 2017.

[21] V. Lokesha, R. Shruti, P. S. Ranjini, and S. Cevik, "On certain topological indices of nanostructures using $Q(G)$ and $R(G)$ perators," *Communications*, vol. 67, pp. 178–187, 2018.

[22] S. Mondal, A. Bhosale, N. De, and A. Pal, "Topological properties of some nanostructures," *Nanosystems: Physics, Chemistry, Mathematics*, vol. 11, no. 1, pp. 14–24, 2020.

[23] M. F. Nadeem, S. Zafar, and Z. Zahid, "On topological properties of the line graphs of subdivision graphs of certain nanostructures," *Applied Mathematics and Computation*, vol. 273, pp. 125–130, 2016.

[24] Y. Shanthakumari, P. Siva Kota Reddy, V. Lokesha, and P. S. Hemavathi, "Topological aspects boron triangular nanotube and boron-α nanotube-II, south east asian," *Journal of Mathematics and Mathematical Sciences (SEAJMMS)*, vol. 16, pp. 145–156, 2020.

[25] S. Iijima, "Synthesis of Carbon Nanotubes," *Nature*, vol. 354, pp. 56–58, 1991.

[26] S. Hayat, M. K. Shafiq, A. Khan et al., "On topological properties of 2-dimensional lattices of carbon nanotubes," *Journal of Computational and Theoretical Nanoscience*, vol. 13, no. 10, pp. 6606–6615, 2016.

[27] A. Ali, W. Nazeer, M. Munir, and M. K. Shin, "M-polynomials and topological indices of zigzag and rhombic benzenoid systems," *Open Chemistry*, vol. 16, pp. 73–78, 2017.

[28] A. Q. Baig, M. Imran, and H. Ali, "Computing omega, sadhana and PI polynomials of benzenoid carbon nanotubes," *Optoelectronics and advanced materials-rapid communications*, vol. 9, pp. 248–255, 2015.
[29] M. Nadeem, A. Yousaf, and A. Razaq, "Certain polynomials and related topological indices for the series of benzenoid graphs," *Scientific Reports*, vol. 9, pp. 1–6, 2019.
[30] F. Harary, *Graph Theory*, Addison-Wesely, Reading Mass, Boston, MA, USA, 1969.
[31] V. R. Kulli, *College Graph Theory*, Vishwa International Publications, Gulbarga, India, 2012.
[32] A. Usha, M. C. Shanmukha, K. N. Anil Kumar, and K. C. Shilpa, "Comparision of novel index with geometric-arithmetic and sum-connectivity indices," *Journal of Mathematical and Computational Science*, vol. 11, pp. 5344–5360, 2021.
[33] D. Vukicevic and B. Furtula, "Topological index based on the ratios of geometric and arithmetical means of end-vertex degrees of edges," *Journal of Mathematical Chemistry*, vol. 46, pp. 1369–1376, 2009.